https://tbj.ui.ac.ir
Taxonomy and Biosystematics
E-ISSN: 3115-9001
Document Type: Research Paper
Vol. 18, Issue 3, No.68, (2026), P:13-28
Received: 04/11/2025 Accepted: 28/12/2025

Research Paper

Morphological characteristics of an isolated population of the cyprinid *C. saadii* (Teleostei: Cyprinidae) from Kavir-e Lut basin in southeastern Iran

Azad Teimori *
Department of Biology, Faculty of Sciences, Shahid Bahonar University of Kerman, Kerman, Iran
a.teimori@uk.ac.ir

Asma Bani Asadi
Department of Biology, Faculty of Sciences, Shahid Bahonar University of Kerman, Kerman, Iran
asmabaniasadi62@gmail.com

Mina Motamedi
Department of Biology, Faculty of Sciences, Shahid Bahonar University of Kerman, Kerman, Iran
m.motamedi@uk.ac.ir

Majid Askari Hesni
Department of Biology, Faculty of Sciences, Shahid Bahonar University of Kerman, Kerman, Iran
mahesni@uk.ac.ir

Abstract
This study investigates the morphology of an isolated population of the cyprinid fish *Capoeta saadii* in the Nesa River within the Lut-Kavir Basin of Iran. Based on an integrated analysis of 52 specimens, the study employed meristic counts, 17 standardized morphometric characters, and seven otolith (asteriscus) morphometric characters. The studied population exhibits distinctive meristic and morphological traits, including 70–86 lateral line scales, 10–14 gill rakers, and disc- or wheel-shaped otoliths with well-developed serrated posterior margins and prominent protuberances. These features morphologically differentiate the Nesa River population from other described populations of *C. saadii* and related species such as *C. fusca*. Sexual dimorphism in meristic traits of the studied population was limited; however, it was evident in several morphometric variables and in otolith morphology, including the interorbital distance and the relative dorsal otolith length. Our findings indicate the presence of a geographically isolated population of *C. saadii* in the Lut-Kavir Basin, which is morphologically distinct and suggests potential adaptations of this riverine population to its desert environment. Robust species delimitation within the *C. saadii* complex requires confirmation from independent nuclear markers and broader comparative data (e.g., the COI gene), which should be addressed in future studies. The escalating environmental threats to the fragile freshwater ecosystems of the Kavir-e Lut Basin necessitate immediate conservation attention for this population, even as its formal taxonomic status awaits future genetic validation.

Keywords: Cryptic species, otolith morphology, morphological variation, desert adaptation, freshwater fish conservation.

*Corresponding author
Teimori, A. , Bani Asadi, A. , Motamedi, M. and Askari Hesni, M. (2026). Morphological characteristics of an isolated population of the cyprinid C. saadii (Teleostei: Cyprinidae) from Kavir-e Lut basin in southeastern Iran. *Taxonomy and Biosystematics*, *18*(3), 13-28.

http://dx.doi.org/10.22108/tbj.2025.147286.1325

Introduction

The genus *Capoeta* Valenciennes, 1842 (family Cyprinidae), comprises 29 valid species distributed across southwestern Asia, including the Levant, Mesopotamia, Turkey, and Iran (Alwan et al., 2016; Fricke et al., 2024). Divergence times for the main *Capoeta* clades in Iranian drainages are estimated at approximately 15.6–12.4 million years ago (Ghanavi et al., 2016). These medium- to large-sized cyprinids possess a compressed to rounded body form, small to moderately large scales, and considerable morphological variability, reflecting adaptations to diverse freshwater habitats (Turan et al., 2022). Historically, all algae-scraping "*Capoeta*-like" fishes were classified within the genus *Capoeta*. Recent molecular and morphological studies, however, have prompted taxonomic revision. Specifically, work by Levin et al. (2012) and Turan et al. (2022) demonstrated that the Mesopotamian group represents a distinct lineage, reclassified into the new genus *Paracapoeta*. This split is supported by genetic distances and key morphological traits, including a strongly ossified last dorsal-fin ray in *Paracapoeta* and distinct scale melanophore patterns (arranged in rows in *Capoeta* versus scattered in *Paracapoeta*) (Turan et al., 2022). The *Capoeta trutta* species group, as defined by Levin et al. (2012), comprises several closely related species, including *C. trutta, C. barroisi, C. erhani, C. mandica*, and *C. turani*, that are distinguished by subtle morphological differences and diagnostic nucleotide substitutions in mitochondrial genes such as COI and Cyt b (Zareian et al., 2016, 2018). Recent discoveries of new species, such as *C. anamisensis* from southern Iran, underscore the genus's unresolved diversity and the necessity of integrative taxonomic methods (Zareian et al., 2016). In Iran, the broader "*Capoeta* group" (including *Paracapoeta*) is highly diversified, represented by 18 species of *Capoeta* and four of *Paracapoeta*, constituting a critical component of the country's freshwater fauna (Fricke et al., 2024). These taxa are found in all major Iranian basins, except the Sistan and Mashkid basins in the southeast (Zareian et al., 2016). The Kavir-e Lut basin in southeastern Iran is an arid, saline environment where extreme ecological conditions likely drive unique adaptations in aquatic fauna. Although *Capoeta fusca* has been documented in this region (Johari et al., 2009), preliminary data indicate the presence of previously unrecognized diversity. During recent fieldwork in the Kavir-e Lut basin of southeastern Iran (Fig. 1), we collected specimens of an algae-scraping cyprinid from the Nesa River, upstream of the Nesa Dam. This population inhabits a remote desert region and has not been included in previous studies (Ghanavi et al., 2016). Based on preliminary morphological examination, we hypothesized that this population belongs to the *C. saadii* species complex. This study tests this hypothesis using an integrative approach to investigate the taxonomic identity of this population from Iran's Kavir-e Lut basin, by combining meristic counts, and detailed morphometrics, including body and otolith morphology. This work provides the first integrative taxonomic assessment, including fish and otolith morphology for this poorly understood population, testing its taxonomic status. The findings contribute to understanding the diversification of *Capoeta* in Iran's desert ecosystems and provide critical data for conservation strategies, as many congeners face escalating threats from habitat degradation and climate change, particularly in arid hotspots like the Kavir-e Lut basin (Geiger et al., 2014).

Materials and Methods

Sampling and initial processing

We collected 52 specimens (20 male, 32 female) from the Nesa River (28°39'51.01"N, 58°19'24.71"E), upstream of the Nesa Dam in Iran’s southeastern Kavir-e Lut basin (Figs. 1-2). Sampling occurred during three periods: November and December 2022 and August 2023, using hand nets. To evaluate the taxonomic distinctiveness of this population, we used a combination of meristic and morphometric data, following the diagnostic criteria for *Capoeta* species delineation (Turan et al., 2006).

http://dx.doi.org/10.22108/tbj.2025.147286.1325

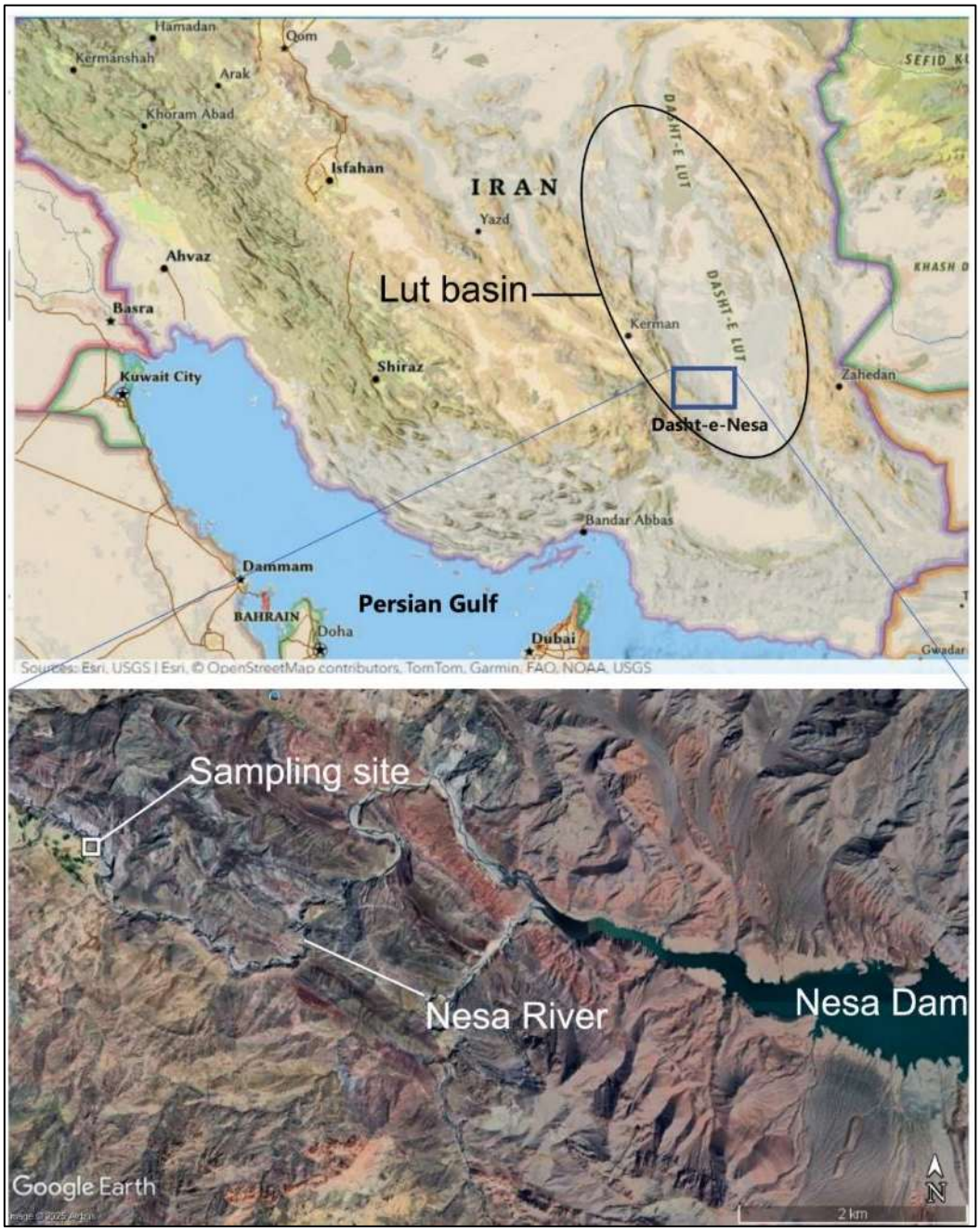

Figure 1. Map of Iran showing the sampling location in the Nesa River, upstream of the Nesa Dam in the Kavir-e Lut basin.

Preservation and examination

Each specimen was cataloged and photographed prior to analysis. Total length (TL) was measured to the nearest millimeter using a digital caliper, from the anterior tip of the head to the posterior margin of the caudal fin lobes. Sex was determined by direct examination of the gonads. Following examination, ten specimens were preserved in 99% ethanol for the analysis of otolith morphology. The remaining specimens were fixed in 10% ethanol and transferred to the laboratory for morphological assessment. Subsequently, all fish specimens were re-preserved in 70% ethanol and deposited in the Zoological Museum of Shahid Bahonar University of Kerman (voucher codes: ZMSBUK-1321 to ZMSBUK-1373). All procedures for handling and euthanizing fish followed the guidelines approved by the Ethics Committee of Shahid Bahonar University of Kerman (ethical approval code: IR.UK.VETMED.REC.1399.010).

Figure 2. Nesa River, in the Kavir-e Lut drainage, southeastern Iran, showing the typical environment of the studied *Capoeta* population.

Otolith extraction and analysis

For the morphometric analysis of the asteriscus (lagenar) otolith, a subset of 34 well-preserved, and undamaged otoliths were selected from the total collection of 52 specimens for detailed morphometrics. This subsample consisted of 22 females and 12 males, ensuring representation across the size range of the collected individuals. We analyzed the asterisci otoliths due to their relatively large size within Cyprinidae and their established taxonomic utility (Assis, 2003; Dörtbudak et al., 2025). Therefore, we employed asteriscus otolith shape as a primary taxonomic character, following the methodological precedent established in otolith-based systematics (Assis, 2003; Dörtbudak et al., 2025). The extraction followed the protocol of Assis (2003): the skull was surgically opened from the dorsal cranial region under the Eschenbach stereo microscope (Carl Roth, Model 33213), the otic capsules were disconnected, and the left and right otoliths were carefully extracted using fine forceps. The extracted otoliths were then washed in 70% ethanol, rinsed in distilled water, and air-dried in Eppendorf tubes for subsequent digital photography and morphological examination. All otoliths have been deposited at ZMSBUK for archival purposes (voucher code: ZMSBUK-530 to ZMSBUK-554). Morphological descriptions of the asterisci are based on the terminology of Assis (2003) and Dörtbudak et al. (2025), as illustrated in Fig. 3.

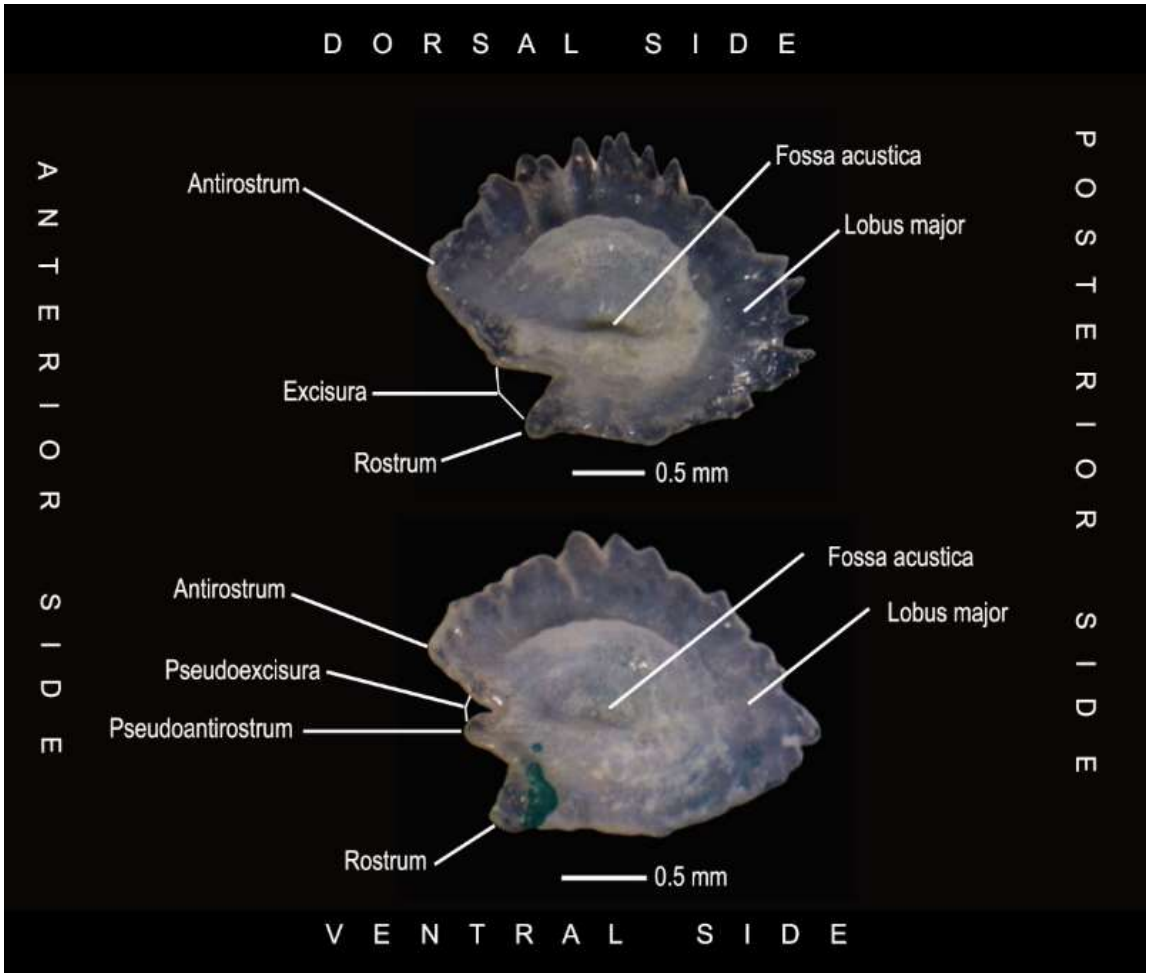

Figure 3. Right asteriscus otolith (medial view) of *Capoeta* from the Nesa River, illustrating the morphological terminology used in the text. Upper otolith: from a 163 mm TL specimen. Lower otolith: from a 165.5 mm TL specimen. Abbreviations: R, rostrum; AR, antirostrum; FA, fossa acustica; LM, lobus major; S, sulcus.

Otolith morphometrics

Seven linear measurements were taken from the asterisci otoliths: antirostrum length, antirostrum height, dorsal length, medial length, rostrum height, otolith length, and otolith height. These measurements were standardized as a function of otolith length and height, respectively. Seven relative otolith variables were then calculated for statistical analysis: relative antirostrum length (R.ant.L), relative antirostrum height (R.ant.H), relative dorsal length (R.dor.L), relative medial length (R.med.L), relative rostrum height (R.ros.H), the length-to-height ratio (L/H), and the ratio of otolith height to standard length (OH/SL).

Fish morphometric and meristic analysis

A total of 52 fish specimens (32 females, 20 males) were analyzed for this study (see Fig. 4 for fish photos). Six meristic traits were counted using an Eschenbach stereo microscope (Carl Roth, Model 33213), and 13 morphometric traits were measured directly using a digital caliper with a precision of 0.05 mm (Table 1). To minimize size-related allometric effects, the morphometric data were standardized related to six reference measurements: standard length (SL), maximum body depth (MaxBD), predorsal distance (PrDD), head length (HL), preanal distance (PrAD), and length of the caudal peduncle (LcauP). From this standardization, 17 relative morphometric variables were derived for subsequent analysis (Table 1).

Table 1. Meristic characters and relative morphometric variables analyzed for the *Capoeta* population from the Nesa River, Kavir-e Lut Basin, southeastern Iran.

Description	Abbreviation
Meristic characters	
The number of unbranched and branched dorsal fin rays	D.fr (unb.fr and b.fr)
The number of unbranched and branched anal fin rays	A.fr (unb.fr and b.fr)
The number of pectoral fin rays	Pec.fr
The number of pelvic fin rays	Pel.fr
Count of gill rakers on the first arch	GR
The number of lateral line scales	LL
Morphometric variables (Standardized using the SL, Maxb, HL, and Prad)	
Total length relative to standard length	TL.SL
Predorsal distance relative to standard length	Prdd.SL
Caudal peduncle length relative to standard length	Lcaup.SL
Body depth relative to standard length	Maxb.SL
Pectoral fin length relative to standard length	Lpef.SL
Dorsal fin length relative to standard length	Ldf.SL
Dorsal fin height relative to maximum body depth	Ddf.Maxb
Head length relative to standard length	HL.SL
Dorsal fin height relative to head length	Ddf.HL
Pectoral fin length relative to head length	Lpecf.HL
Preorbital distance relative to head length	Prod.HL
Post-dorsal distance relative to standard length	Podd.SL
Preanal distance relative to standard length	Prad.SL
Preorbital distance relative to standard length	Prod.SL
Pectoral fin length relative to preanal distance	Lpecf.Prad
Predorsal distance relative to preanal distance	Prdd.Prad
Caudal peduncle length relative to preanal distance	Lcaup.Prad

Figure 4. *Capoeta* specimens from the Nesa River, Kavir-e Lut Basin, southeastern Iran, preserved in 70% ethanol. (a) male, 31.5 cm TL (voucher ZMSBUK-1335); (b, c) females, 29.4 cm and 31.0 cm TL (vouchers ZMSBUK-1365, ZMSBUK-1366, respectively).

http://dx.doi.org/10.22108/tbj.2025.147286.1325

Statistical analyses

Prior to analysis, the assumption of normality was assessed for all 17 fish morphometric variables using the Shapiro-Wilk test. As the majority significantly deviated from normality ($p < 0.05$), non-parametric Mann-Whitney U tests were employed for all comparisons between sexes. Descriptive statistics (mean ± SD, range, and coefficient of variation) were calculated to summarize these population-level traits. To examine otolith morphometric variation, a Principal Component Analysis (PCA) was performed on the seven standardized otolith variables. The PCA was conducted on the correlation matrix using the prcomp function in R (v4.3.0). Components with eigenvalues >1 (Kaiser-Guttman criterion) were retained, accounting for 78.4% of the cumulative variance. Variable loadings with an absolute value ≥ 0.5 were considered significant for interpreting each component. Sexual dimorphism in otolith morphology was further investigated by comparing the PC scores (PC1 and PC2) between sexes using Welch's t-test, with effect sizes quantified by Cohen's d. The results were visualized using PC1-PC2 biplots with 95% confidence ellipses and sex-specific boxplots of the component scores, generated with ggplot2 (v3.4.0). Finally, the distribution of all otolith variables was visualized using combined kernel density and boxplots. These plots, created with ggplot2 in R, overlay a kernel density estimate (violin shape) with a traditional boxplot (showing the median, quartiles, and 1.5× IQR whiskers). This approach highlights central tendency, dispersion, and potential multimodal patterns. Densities were normalized to allow direct comparison across variables, and all outliers were retained to reflect natural morphological variation.

Results

Fish meristic and morphometric characters

The total length (TL) of the examined specimens ranged from 147.7 mm to 283.2 mm. No significant differences were observed between males and females for any of the six meristic traits analyzed (Table 2**)**. The ranges and means for key traits were as follows: pelvic fin rays (males: 8–9, mean 8.93 ± 0.27; females: 9–10, mean 9.22 ± 0.42), dorsal soft fin rays (males: 8–9, mean 8.29 ± 0.72; females: 6–10, mean 8.19 ± 0.94), and lateral line scales (males: 72–83, mean 77.07 ± 3.19; females: 70–86, mean 76.53 ± 3.45). Anal fin rays consisted of 1–2 unbranched rays followed by 5–8 branched rays in both sexes. Gill raker counts were 10–14 (mean 11.71 ± 0.73) in males and 11–14 (mean 12.09 ± 0.89) in females.

Table 2. Meristic counts for male and female *Capoeta* specimens from the Nesa River population. Values are presented as mean ± standard deviation (range: min–max).

Meristic trait	Males (N=20)	Females (N=32)
D.fr (unb.fr)	3.79 ± 0.43 (3–4)	3.72 ± 0.46 (3–4)
D.fr (br.)	8.71 ± 0.47 (8–9)	8.47 ± 0.95 (6–10)
A.fr (unb.fr)	1.58 ± 0.05 (1–2)	1.63 ± 0.49 (1–2)
A.fr (br.)	6.29 ± 0.73 (5–8)	6.19 ± 0.64 (5–8)
Pec.fr	16.93 ± 0.83 (16–18)	16.72 ± 1.59 (12–18)
Pel.fr	8.93 ± 0.27 (8–9)	9.22 ± 0.42 (9–10)
Count of gill rakers	11.71 ± 0.73 (10–13)	12.09 ± 0.89 (11–14)
The number of lateral line scales	77.07 ± 3.45 (72–83)	76.53 ± 3.19 (70–86)

Frequency distribution of meristic counts for male and female *Capoeta* specimens from the Nesa River population are shown in Table 3. For several features, the counts were identical between sexes: the majority of specimens possessed four unbranched dorsal fin rays (D.fr (unb.)) and six branched anal fin rays (A.fr (br.)), while all males and a majority of females exhibited two unbranched anal fin rays (A.fr (unb.)). Females exhibited a wider range and higher counts for several traits, including the presence of six and seven branched dorsal fin rays, ten pelvic fin rays, and gill raker (GR) counts extending to 14.

Table 3. Frequency distribution of meristic counts for male and female *Capoeta* specimens from the Nesa River population. Values are presented as percentages with sample sizes in parentheses.

Trait	Frequency	Males	Females	Trait	Frequency	Males	Females
D.fr (unb.)	3	21.4% (n=6)	28.1% (n=9)	**A.fr (br.)**	5	7.1% (n=2)	9.4% (n=3)
	4	78.6% (n=14)	71.9% (n=23)		6	64.3% (n=12)	65.6% (n=21)
D.fr (br.)	6	–	6.3% (n=2)		7	21.4% (n=4)	21.9% (n=7)
	7	–	6.3% (n=2)		8	7.1% (n=2)	3.1% (n=1)
	8	28.6% (n=7)	28.1% (n=9)	**Pel.fr**	8	7.1% (n=4)	–
	9	71.4% (n=13)	53.1% (n=17)		9	92.9% (n=16)	78.1% (n=25)
	10	–	6.3% (n=2)		10	–	21.9% (n=7)
A.fr (unb.)	1	–	37.5% (n=12)	**GR**	10	7.1% (n=2)	–
	2	100% (n=20)	62.5% (n=20)		11	21.4% (n=4)	28.1% (n=9)
					12	64.3% (n=12)	40.6% (n=13)
					13	7.1% (n=2)	25.0% (n=8)
					14	–	6.3% (n=2)

Frequency of Lateral line scales (LL): Males: 72 (7.1%, n=1), 73 (14.3%, n=2), 74 (7.1%, n=1), 75 (7.1%, n=1), 76 (14.3%, n=2), 78 (7.1%, n=1), 79 (21.4%, n=3), 80 (7.1%, n=1), 82 (7.1%, n=1), 83 (7.1%, n=1), Females: 70 (3.1%, n=1), 72 (6.3%, n=2), 73 (9.4%, n=3), 74 (3.1%, n=1), 75 (12.5%, n=4), 76 (15.6%, n=5), 77 (18.8%, n=6), 78 (9.4%, n=3), 79 (9.4%, n=3), 80 (3.1%, n=1), 81 (3.1%, n=1), 82 (3.1%, n=1), 86 (3.1%, n=1).

Furthermore, the frequency distribution of lateral line scales showed a broader range in females (70-86) compared to males (72-83), indicating slightly greater variability in this meristic character among female specimens. Morphometric analysis revealed significant sexual dimorphism in only two of the 17 relative traits analyzed (Mann-Whitney U test, $p < 0.05$; Table 4). Females exhibited a significantly greater preorbital distance (Prod.SL), with a mean of 9.46% SL (± 0.65), compared to 9.04% SL (± 0.54) in males. Females also had a greater maximum body depth (Maxb.SL) and showed higher variability in this trait (range: 19.16–29.01% SL, mean: 23.69% SL ± 1.78) compared to males (range: 21.88–24.54% SL, mean: 22.77% SL ± 0.89). The remaining 14 morphometric variables, encompassing body proportions (e.g., TL.SL, Lcaup.SL), fin dimensions (Ldf.SL, Lpecf.SL), and head dimensions (HL.SL, Ddf.HL), showed no significant differences between the sexes (Mann-Whitney U test, $p > 0.05$; Table 4).

Table 4. Descriptive statistics analysis of morphometric variables for female (♀) and male (♂) *Capoeta* specimens from the Nesa River population. Values represent range (mean ± standard deviation). Statistical significance was assessed using the Mann-Whitney U test ($p < 0.05$).

VARIABLE	♀ (N = 32)	♂ (N = 20)	MANN-WHITNEY U	P-VALUE
AS % OF SL				
TL.SL	112.86-130.51 (119.55±3.85)	104.72-124.64 (118.26±4.8)	207.00	0.57
PRDD.SL	45.94-57.73 (49.67±2.60)	47.31-55.06 (49.82±2.20)	212.00	0.65
LCAUP.SL	20.11-27.30 (22.73±1.75)	20.60-25.32 (22.69±1.50)	223.00	0.85
MAXB.SL	19.16-29.01 (23.69±1.78)	21.68-24.54 (22.77±0.89)	147.00	0.05
LPECF.SL	14.12-21.79 (19.99±1.43)	13.24-23.06 (19.82±2.23)	213.00	0.67
LDF.SL	13.27-19.78 (14.96±1.10)	11.73-16.73 (14.67±1.23)	211.00	0.64
DDF.MAXB	54.03-108.49 (81.04±10.50)	71.91-93.62 (83.95±6.27)	179.00	0.22
HL.SL	21.53-27.31 (24.06±1.47)	21.99-25.28 (23.35±1.12)	164.00	0.11
PODD.SL	48.77-60.89 (55.27±2.63)	53.17-64.10 (56.44±2.84)	194.00	0.38
PRAD.SL	68.05-92.25 (83.92±4.46)	67.75-81.65 (73.27±3.11)	214.00	0.69
PROD.SL	7.52-10.40 (9.46±0.65)	7.92-9.92 (9.04±0.54)	126.00	**0.01**
AS % OF HL				
DDF.HL	55.78-91.48 (79.44±7.50)	73.81-88.55 (81.79±4.56)	184.000	0.274
LPECF.HL	63.85-91.20 (83.22±5.68)	59.31-94.90 (83.84±8.52)	172.000	0.170
PROD.HL	33.27-279.30 (46.62±41.82)	33.81-43.45 (38.75±2.56)	196.000	0.416
AS % OF PRAD				
LPECF.PRAD	19.04-29.34 (27.11±2.09)	19.55-30.93 (27.00±2.43)	204.000	0.530
PRDD.PRAD	55.84-75.80 (67.32±3.60)	63.72-73.49 (68.02±2.46)	206.000	0.561
LCAUP.PRAD	22.28-36.00 (30.82±2.43)	27.68-35.39 (30.99±2.00)	226.000	0.907

Morphological description of asterisci otoliths

The morphology of asterisci otoliths was consistent between sexes, with no visually discernible dimorphic features; representative otoliths for males and females are shown in Figures 5 and 6, respectively. All examined otoliths were classified as paramedian, with the pseudoexcisura tip positioned above the midline axis.

General shape and surfaces

The otoliths exhibited a discoid (asteriform) shape, rounded in medial view. The surface was characterized by prominent protuberances at the anterior and posterior ends, with fewer protrusions along the mid-region (Fig. 5a,d,i,j; Fig. 6b,c,d,h,i). The medial surface was consistently concave, while the opposite surface was convex.

Marginal descriptions

Dorsal margin: Displayed serrations that extended to the posteroventral region, with considerable individual variation in size and number.

Ventral margin: Predominantly smooth, often featuring an anterior swell (Fig. 5a,b,i; Fig. 6h,i). A subset of otoliths exhibited short protuberances on the posterior ventral margin (Fig. 5b,c,g; Fig. 6c,e,h).

Anterior margin: Varied in form, ranging from straight to slightly pointed (Fig. 5a,c,f,k; Fig. 6b,c,h,j,k) or oblique (Fig. 5b,g,j; Fig. 6a,e,f,i).

Posterior margin: Typically rounded and furnished with short protuberances. These protuberances were absent or weakly developed in a minority of specimens (Fig. 5c,e; Fig. 6g,j,k).

http://dx.doi.org/10.22108/tbj.2025.147286.1325

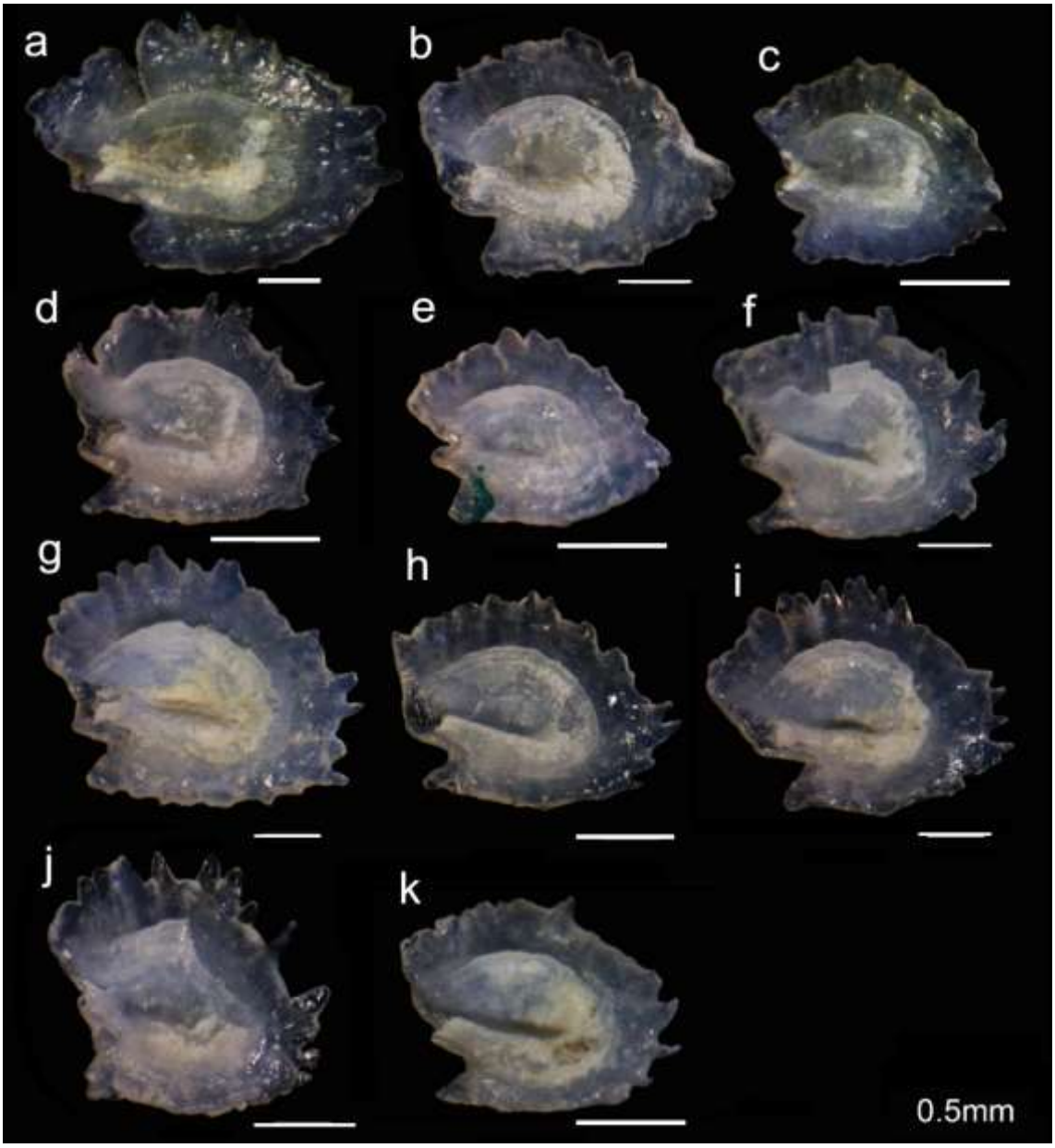

Figure 5. Right asterisci otoliths (medial view) for male specimens collected from the Nesa River. Otolith vouchers are provided in the materials and method section.

Distinct morphological features

Rostrum: Typically short and pointed. A short, blunt morphology was observed in two instances (Fig. 5a,b; Fig. 6b).

Antirostrum: Generally slightly oblique with a rounded tip. This feature was poorly developed and emergent in two otoliths (Fig. 5h,k).

Pseudoantirostrum: Not well-developed; it was small with a narrow, rounded to pointed tip. A distinct pseudoantirostrum was absent in several specimens (Fig. 5a,b,h,i-k; Fig. 6h).

Pseudoexcisura: Mostly indistinct. When present, it was either wide and shallow (Fig. 5a,c,d,g; Fig. 6a,b,d-f,g,j) or deep and narrow (Fig. 5e,f).

Fossa acustica: Consistently wide and deep, with a predominantly round and rarely elliptical shape.

Lobus major: Appeared crumpled in lateral view and was covered with variable-sized and shaped deposits.

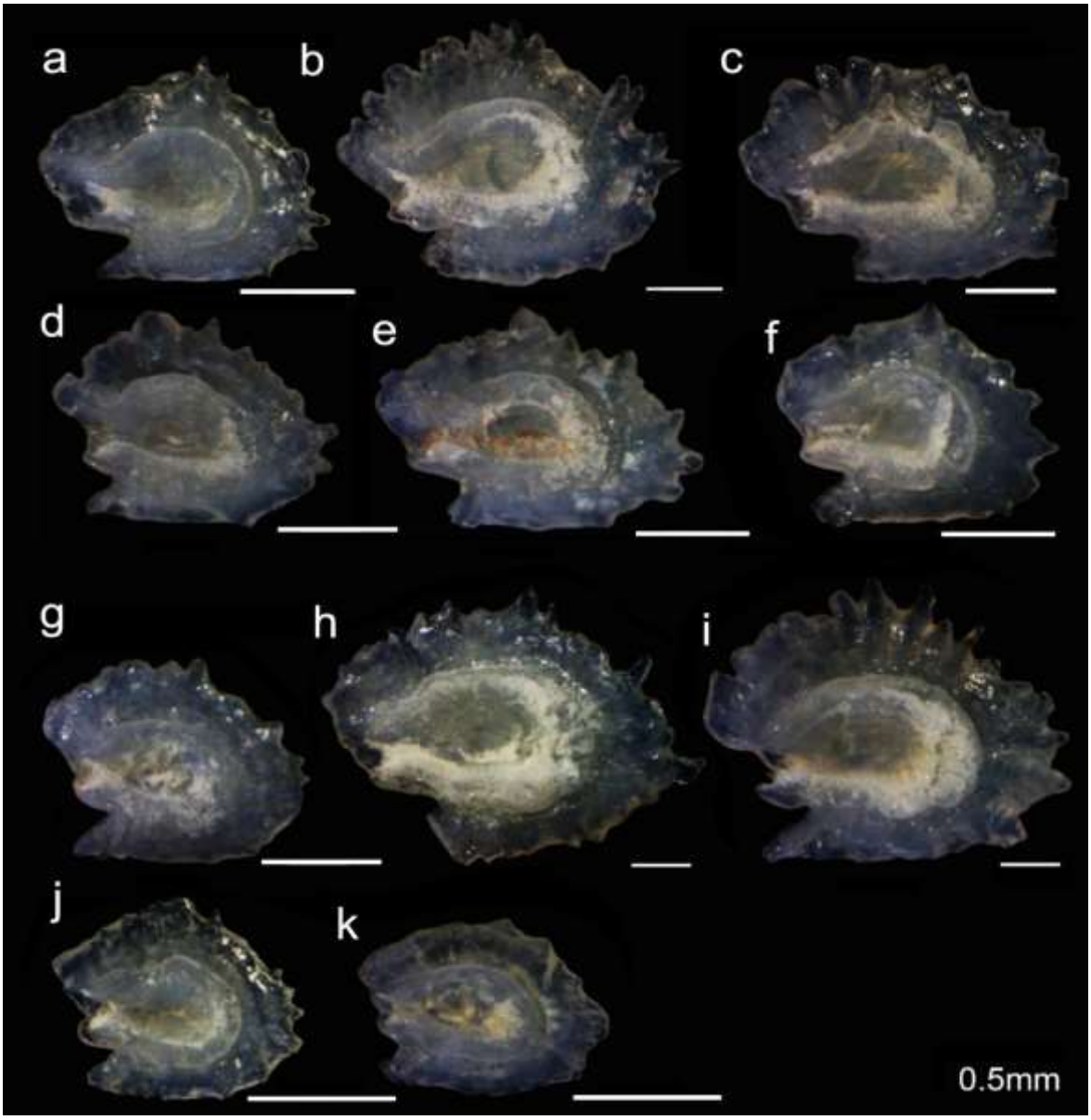

Figure 6. Right asterisci otoliths (medial view) for female specimens collected from the Nesa River. Otolith vouchers are provided in the materials and method section.

Analysis of otolith morphometrics

Descriptive statistics and Mann-Whitney U test results for otolith morphometric variables are presented in Table 5. Females generally exhibited greater variability (higher standard deviation) in otolith dimensions, particularly in the relative dorsal length (R.dor.L). Females exhibited larger mean values than males in most otolith variables, including the relative dorsal length (R.dor.L: 138.69 ± 12.52 in female vs. 120.84 ± 10.72 in male), relative medial length (R.med.L: 130.65 ± 11.56 in female vs. 120.55 ± 12.41 in male), and length-height index (L/H: 126.32 ± 11.41 in female vs. 114.81 ± 10.92 in male). The males showed slightly greater relative rostrum height (R.ros.H: 38.65 ± 5.79 in male vs. 36.54 ± 9.08 in female). The Mann-Whitney U test results revealed significant sexual dimorphism in the relative dorsal length (R.dor.L) (U=154.00, p=0.03), with females exhibiting longer dorsal length in their otoliths (138.69 ± 12.52) compared to males (120.84 ± 10.72), and in the relative antirostrum length (R.ant.L) (p=0.05) (Table 5). The remaining variables displayed no significant difference between the sexes (p>0.05). Principal Component Analysis (PCA) of otolith morphometric variables revealed subtle but apparent morphological differences between sexes (Fig. 7).

http://dx.doi.org/10.22108/tbj.2025.147286.1325

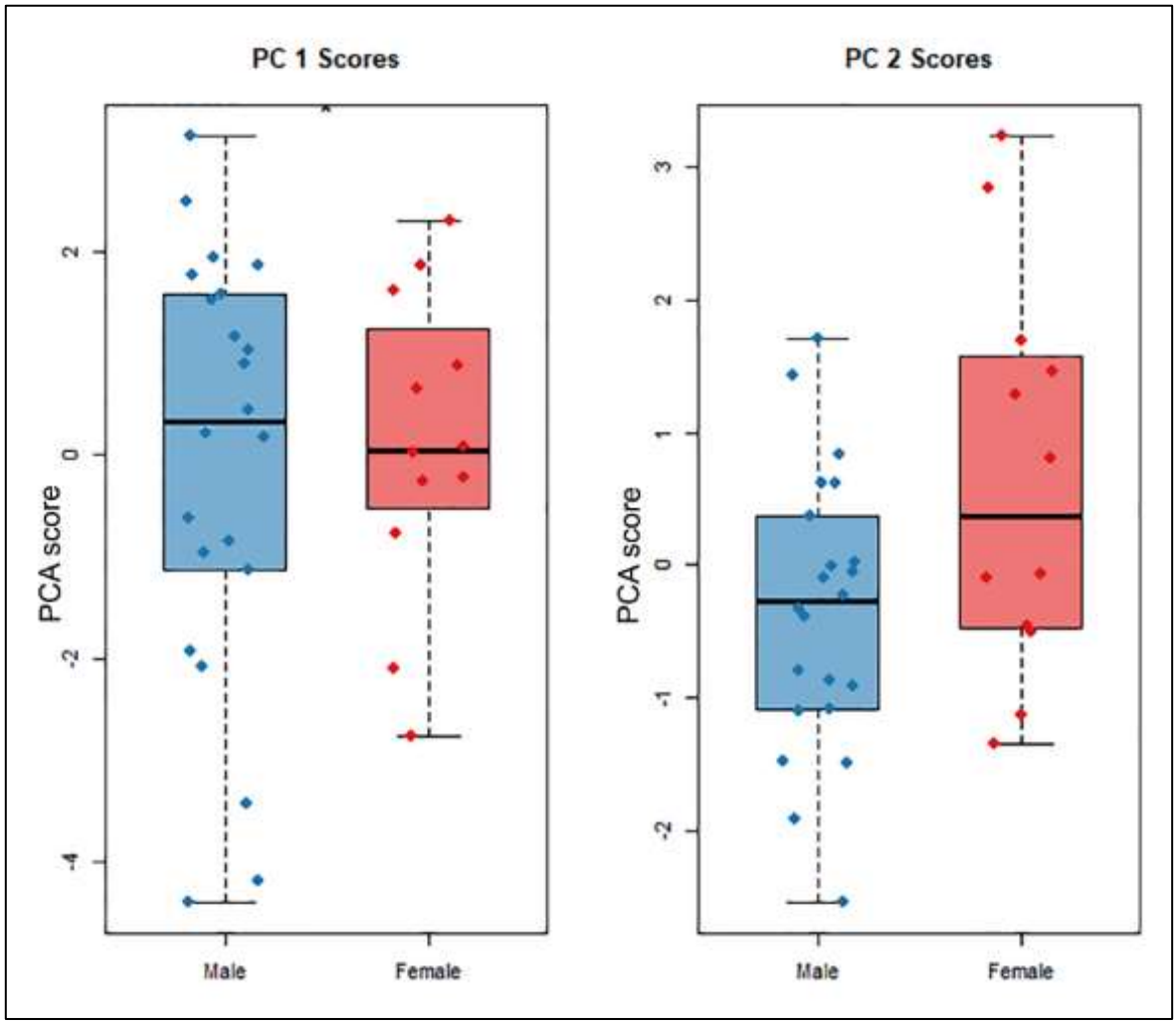

Figure 7. PCA scores plot of otolith morphometric variables for male and female *Capoeta* from the Nesa River. Each point represents an individual otolith positioned by its scores on Principal Components 1 and 2 (PC1, PC2).

The scatter plot of PC1 versus PC2 showed partial overlap between the male and female distributions. However, females tended to cluster toward higher PC1 scores, indicating greater variability in otolith features linked to this component (e.g., relative dorsal length, which differed significantly, Mann-Whitney test, $p<0.05$). In contrast, males exhibited marginally higher dispersion along PC2.

Kernel density analysis

The kernel density estimation of six otolith shape indices revealed distinct morphological distributions (Fig. 8). The density curves for Relative Rostrum Height (R.ros.H) and Relative Antirostrum Height (R.ant.H) were notably tall and narrow, indicating very constrained distributions and low variability within the population. In contrast, the curve for the Length-to-Height ratio (L/H) was the shortest and broadest. The distributions for Relative Dorsal Length (R.dor.L), Relative Medial Length (R.med.L), and Relative Antirostrum Length (R.ant.L) displayed intermediate widths. Furthermore, the distribution for Relative Dorsal Length (R.dor.L) showed a clear right-skew, indicating a tendency toward larger values.

Table 5. Descriptive statistics and results of Mann-Whitney U test for otolith morphometric variables in female (n=22) and male (n=12) *Capoeta* specimens. Values are presented as min–max (mean ± standard deviation). Variables showing significant sexual dimorphism ($p < 0.05$) are indicated in bold. Abbreviations: R.ant.L (Relative antirostrum length), R.ant.H (Relative antirostrum height), R.dor.L (Relative dorsal length), R.med.L (Relative medial length), R.ros.H (Relative rostrum height), L/H (Length/Height ratio), OH/SL (Otolith height/Standard length ratio).

Variable	Min-Max (Mean±SD)		Mann-Whitney U	p-value
	♀	♂		
R.ant.L	**5.31-31.32 (20.27±5.83)**	**4.68-31.43 (17.33±6.76)**	160.00	**0.05**
R.ant.H	25.99-66.03 (40.67±9.26)	21.13-55.77 (41.10±8.86)	239.00	0.22
R.dor.L	**100.55-192.62 (138.69±12.52)**	**83.76-177.32 (120.84±10.72)**	154.00	**0.03**
R.med.L	94.92-184.07 (130.65±11.56)	84.96-169.36 (120.55±12.41)	165.00	0.11
R.ros.H	25.52-67.85 (36.54±9.08)	30.67-46.52 (38.65±5.79)	247.00	0.18
L/H index	1.08-1.51 (1.27±0.15)	0.93-1.39 (1.26±0.12)	206.00	0.90
OH.SL	0.91-1.55 (1.23±0.16)	1.11-1.28 (1.20±0.06)	198.00	0.67

Discussion

Morphological differentiation, and taxonomic implications

Our study, combining meristic, morphometric, and otolith morphology, provides compelling evidence that the *Capoeta* population from the isolated Nesa River represents a differentiated lineage within the *C. saadii* complex. The meristic data obtained for the *Capoeta* population from the Nesa River reveal a morphological profile that allows for comparative discussion with related taxa. The population shows a notable affinity with certain members of the genus *Capoeta*, particularly *C. buhsei* (Yazdani et al., 2016) and *C. saadii* (Zareian et al., 2016), as evidenced by highly overlapping ranges for lateral line scales (LL: 70–86 vs. 72–91 and 65–75, respectively) and nearly identical dorsal and anal fin ray formulae (this study). However, it can be differentiated from other congeners, such as *C. fusca*, which possesses a markedly lower lateral line scale count (42–62; Johari et al., 2009), and *C. ferdowsii*, which exhibits a higher number of branched dorsal and anal fin rays (Jouladeh-Roudbar et al., 2017). The most pronounced morphological disparity is observed when comparing the Nesa population to species of the genus *Paracapoeta*. The gill raker count (GR: 10–14) for the Nesa population is substantially lower than that of both *P. mandica* (23–27; Zareian et al., 2018) and *P. trutta* (23–33; Keivany et al., 2016), a key diagnostic trait that suggests significant divergence in feeding ecology and phylogenetic placement (see also Table 6).

Table 6. Comparative meristic data for *Capoeta* population from the Nesa River and related species of genera *Capoeta* and *Paracapoeta* from Iran.

Species	D.fr (unb./br.), Afr. (unb./br.), LL, GR, Pel.fr	References
Nesa River population	3–4 / 6–10, 1–2 / 5–8, 70–86, 10–14, 8–10	This study
C. saadii	3-4 / 8–9, 3 / 5, 65–75, 9–16, 8–10	Zareian et al. (2016)
C. fusca	3 / 7–8, 3 / 5, 42–62, 11–20, 7–9	Johari et al. (2009)
C. buhsei	3-4 / 8–9, 3 / 5, 72–91, 11–13, 7–9	Yazdani et al. (2016)
C. ferdowsii	3–4 / 12–13, 3 / 8, 68–77, 15–18 ,9–10	Jouladeh-Roudbar et al. (2017)
P. mandica	3-4 / 7–8, 3 / 5, 58–68, 23–27 / 7–8	Zareian et al. (2018)
P. trutta	3 / 7–9, 2-3 / 4–6, 68–90, 23–33, 6–8	Keivany et al. (2016)

This combination of similarities with specific *Capoeta* species and clear discontinuities with others, especially *Paracapoeta*, provides strong morphological evidence for its classification within the genus *Capoeta* and highlights its unique identity, warranting further investigation into its precise taxonomic status. The observed otolith differences are based on a comparative description relative to its examined relatives (*C. saadii*) and to the available descriptions of *C. fusca* in the literature (Askari Hesni et al., 2020). The most prominent morphological differences were found in the asteriscus otoliths. The otoliths of the Nesa River population are characterized by a unique discoid/gyro-type shape with strongly serrated dorsal margins and large anterior and posterior protuberances (Figs. 5-6). This morphology is markedly different from the slightly serrated otoliths of *C. fusca* (Fig. 9a-d) and the smooth or faintly undulating margins of *C. saadii* (Fig. 9e-h). The otolith morphology of the Nesa River population exhibits distinctive characteristics that clearly differentiate it from the compared congeners, *C. fusca* and *C. saadii*. The overall shape is notably more robust and rounded, being described as discoid/gyro-type with thick margins, in contrast to the oval form of *C. fusca* (Askari Hesni et al., 2020), and the elongated, slender otoliths of *C. saadii* (Table 7). A key characteristic for the Nesa population is the presence of strongly serrated dorsal margins, a feature, which is only slightly serrated in *C. fusca* and smooth or faintly undulating in *C. saadii*. Furthermore, the Nesa otoliths possess large, prominent protuberances on the anterior and posterior regions, which are either small and evenly spaced in *C. fusca* or largely absent in *C. saadii*. Additional distinguishing features include a consistently short and pointed rostrum, a well-developed oblique antirostrum, and a particularly wide and deep fossa acustica. Finally, the surface of the lobus major shows a characteristically crumpled and irregular texture, providing a further point of differentiation from the slightly textured surface in *C. fusca* and the smooth surface in *C. saadii* (Table 7).

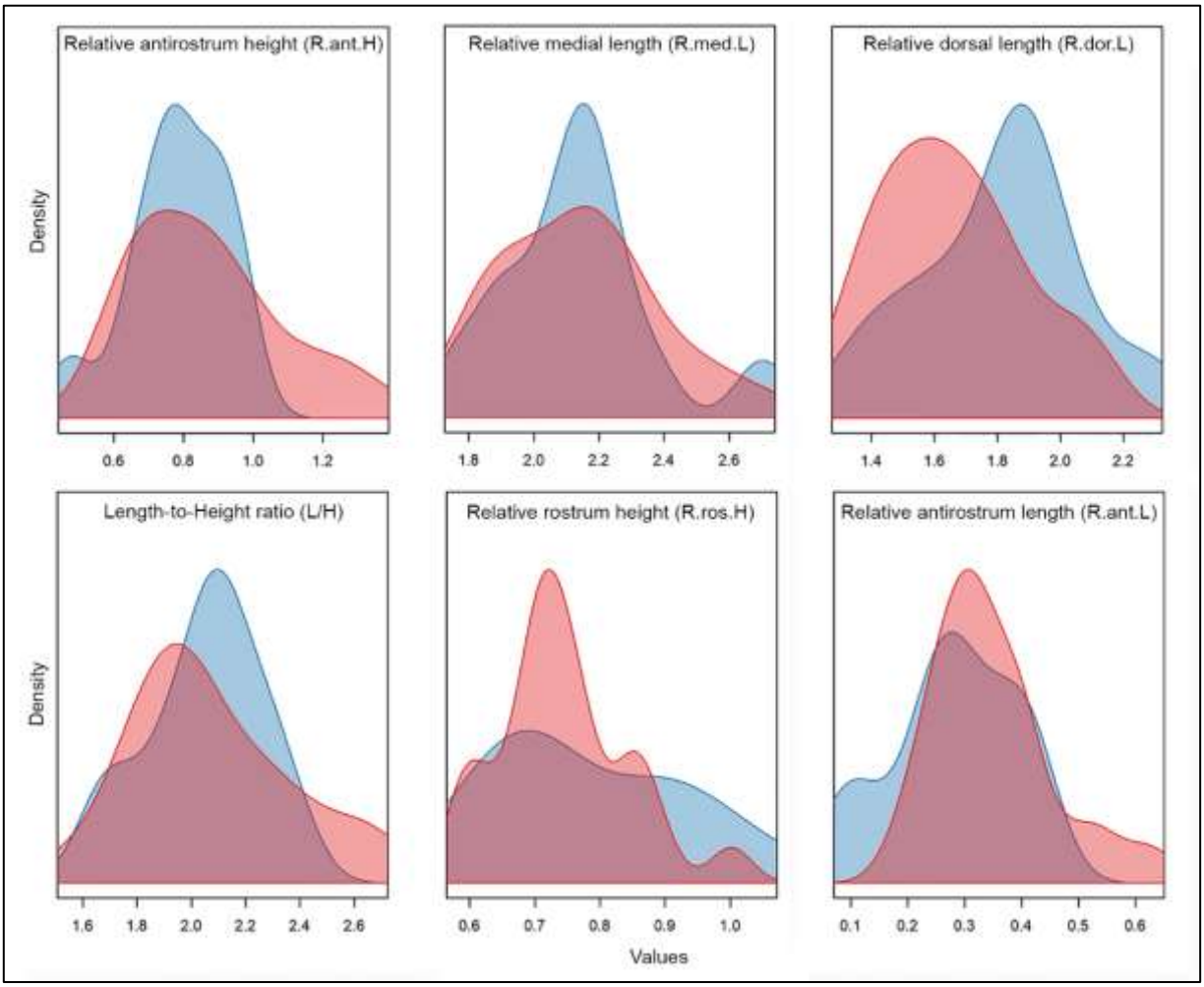

Figure 8. Kernel density distributions of six standardized otolith morphometric variables for the *Capoeta* population from the Nesa River. Plots show the distribution for Relative antirostrum height (R.ant.H), Relative medial length (R.med.L), Relative dorsal length (R.dor.L), Length-to-Height ratio (L/H), Relative rostrum height (R.ros.H), and Relative antirostrum length (R.ant.L).

Table 7. Comparison of otolith morphology among Nesa River population, *C. saadii*, and *C. fusca*, highlighting diagnostic features of the otolith among three close taxa.

Otolith feature	Nesa River population (Figs. 5-6)	*C. fusca* (Fig. 9a-d)	*C. saadii* (Fig. 9e-h)	Comparative remarks
Overall shape	Discoid/gyro-type, thick margins	Oval, moderately thick	Elongated, slender	*Capoeta* sp. more robust and rounded than the others.
Margins	Strongly serrated (dorsal edge)	Slightly serrated	Smooth or faintly undulating	Serrations are a key characteristic for *Capoeta* sp.
Protuberances	Large, anterior/posterior	Small, evenly spaced	Absent or minimal	Protuberances in *Capoeta* sp. are unique in size and placement.
Rostrum	Short, pointed (rarely blunt)	Short to moderate, variable	Weak or indistinct	Rostrum more prominent and consistent in *Capoeta* sp.
Antirostrum	Oblique, rounded tip	Moderately defined	Poorly developed	Better developed in *Capoeta* sp. vs. *C. saadii*.
Fossa acustica	Wide and deep, round	Moderately deep	Narrow, shallow	Fossa shape is distinctively expansive in *Capoeta* sp.
Lobus major	Crumpled, irregular depositions	Slightly textured	Smooth	*Capoeta* sp. shows greater surface complexity.

Otolith morphology has been established as a valuable taxonomic tool in cyprinids, often revealing cryptic diversity and species-specific signatures linked to genetic divergence and habitat (Assis, 2003; Salehi Nejad Ranjbar et al., 2016; Dörtbudak et al., 2025). From a biogeographic perspective, the isolation of the Kavir-e Lut Basin, characterized by extreme aridity, high salinity, and elevated temperatures, has likely acted as a formidable dispersal barrier. This scenario of hydrological fragmentation driving allopatric speciation

is a common theme in the diversification of arid-region freshwater fishes. Similar patterns of isolated basins harboring unique lineages have been documented in the *Garra* species flock of the Arabian Peninsula (Geiger et al., 2014) and in the cichlid *Iranocichla* in southern Iran (Esmaeili et al., 2016). The Miocene-Pliocene uplift of the Zagros Mountains and subsequent aridification events have been major drivers of vicariance in southwestern Asian freshwater fishes (Ghanavi et al., 2016). The observed variation in the morphological characteristics of the Nesa River population likely reflect such historical processes, mirroring the divergence observed in the Mesopotamian *Paracapoeta* (Turan et al., 2022) and *Labeobarbus* (Beshera & Harris, 2014), where desert basins served as evolutionary traps and cradles. Given the congruent evidence, the question of its taxonomic status arises. The possession of a suite of unique, diagnosable morphological traits (e.g., otolith architecture, caudal peduncle length) suggests considerable differentiation of the studied population. However, in line with a cautious and integrative approach for this complex group, we explicitly refrain from any formal taxonomic description here until we provide the molecular data of COI gene for species delimitation combined with nuclear markers. As demonstrated in other cyprinid studies, mitochondrial trees can sometimes be confounded by past introgression or incomplete lineage sorting (e.g., Perea et al., 2010). Robust species delimitation within the *C. saadii* complex requires confirmation from independent nuclear markers and broader comparative data (e.g., the COI gene), which should be addressed in future studies. The escalating environmental threats to the fragile freshwater ecosystems of the Kavir-e Lut Basin necessitate immediate conservation attention for this population, even as its formal taxonomic status awaits future genetic validation.

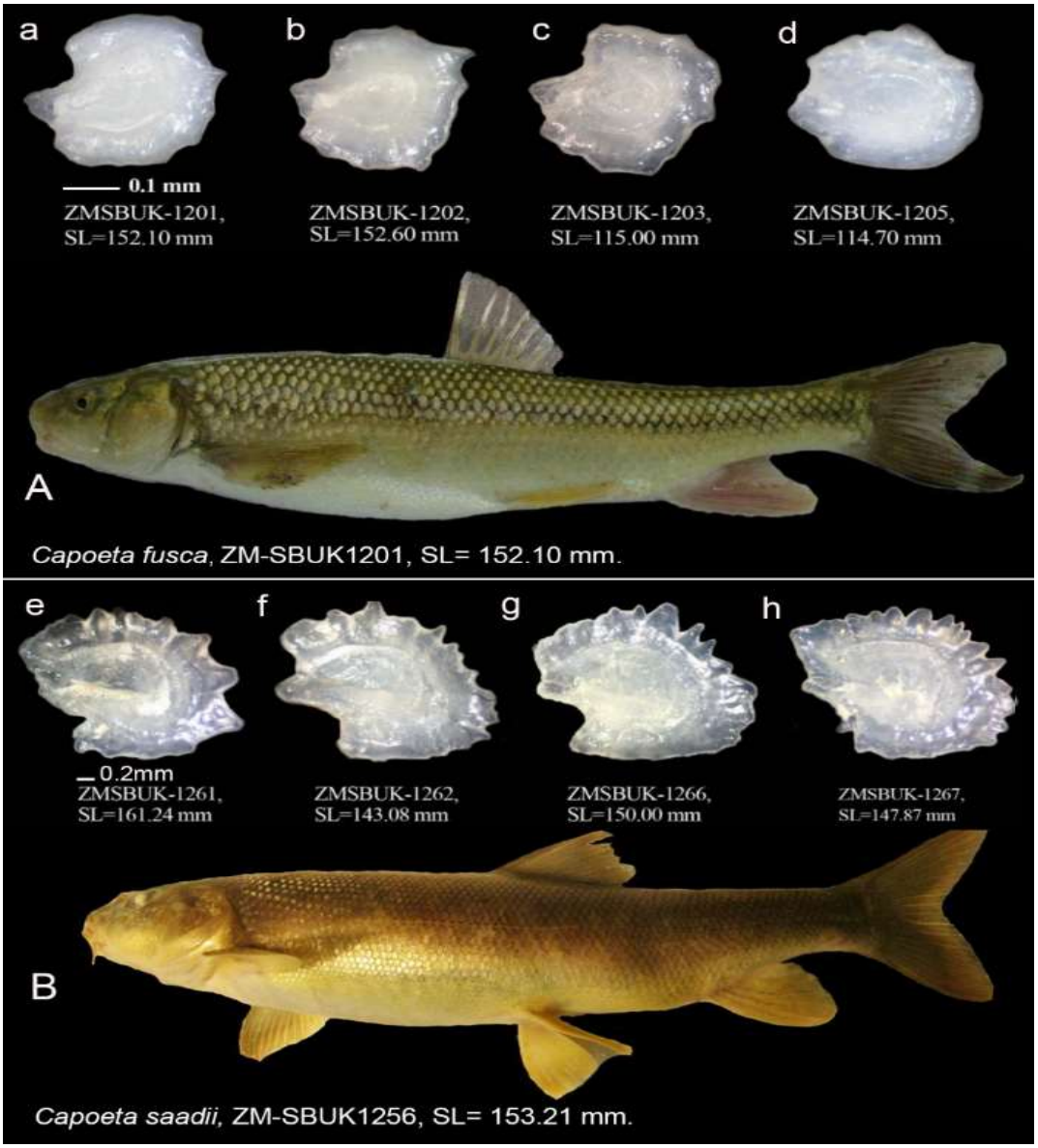

Figure 9. Comparative asteriscus otolith morphology (medial view) of (A) *Capoeta fusca* (a-d) and (B) *Capoeta saadii* (e-h). Specimen catalog numbers and standard lengths (SL) are provided for each otolith. The otoliths of *C. fusca* are from Askari Hesni et al. (2020).

http://dx.doi.org/10.22108/tbj.2025.147286.1325

Data availability

The data that support the findings of this study are available from the corresponding authors upon reasonable request.

Declaration of competing interest

The authors declare that they have no known competing financial interests or personal relationships that could have appeared to influence the work reported in this paper.

Acknowledgments

We would like to thank local people in the sampling site for their kind assistance in fish collection and logistic actions.

Funding Information

This study was funded by the grant received from Shahid Bahonar University of Kerman to the first author (Grant number A134203).

References

Alwan, N., Zareian, H., & Esmaeili, H. R. (2016). *Capoeta coadi*, a new species of cyprinid fish from the Karun River drainage, Iran based on morphological and molecular evidences (Teleostei, Cyprinidae). *ZooKeys*, *572*, 155–180. https://doi.org/10.3897/zookeys.572.7377

Askari Hesni, M., Mohammadi, F., Teimori, A., & Madjdzadeh, S. M. (2020). The intraspecific variations of otolith and urohyal bone structures in *Capoeta fusca* (Nikolskii, 1897) (Teleostei: Cyprinidae) in Loot Basin. *Journal of Animal Research*, *33*(2), 153–167. https://animal.ijbio.ir/article_1642_en.html [In Persian]

Assis, C. A. (2003). The lagenar otoliths of teleosts: Their morphology and its application in species identification, phylogeny and systematics. *Journal of Fish Biology*, *62*(6), 1268–1295. https://doi.org/10.1046/j.1095-8649.2003.00106.x

Beshera, K. A., & Harris, P. M. (2014). Mitochondrial DNA phylogeography of the *Labeobarbus intermedius* complex (Pisces, Cyprinidae) from Ethiopia. *Journal of Fish Biology*, *85*(2), 228-245. https://doi.org/10.1111/jfb.12408

Dörtbudak, M. Y., Demiraslan, Y., Demircioğlu, İ., & Aksünger Karaavcı, F. (2025). Shape analysis of otoliths of *Capoeta trutta* (Heckel, 1843) and *Capoeta umbla* (Heckel, 1843) species by geometric morphometry. *Erciyes Üniversitesi Veteriner Fakültesi Dergisi*, *22*(1), 7–12. https://doi.org/10.32707/ercivet.1540573

Esmaeili, H. R., Sayyadzadeh, G., & Seehausen, O. (2016). *Iranocichla persa*, a new cichlid species from southern Iran (Teleostei, Cichlidae). *ZooKeys*, *636*, 141–161. https://doi.org/10.3897/zookeys.636.10571

Fricke, R., Eschmeyer, W. N., & Van der Laan, R. (Eds.). (2024). *Eschmeyer's Catalog of Fishes: Genera, species, references*. Retrieved June 25, 2024, from http://researcharchive.calacademy.org/research/ichthyology/catalog/fishcatmain.asp

Geiger, M. F., Herder, F., Monaghan, M. T., Almada, V., Barbieri, R., Bariche, M., Berrebi, P., Bohlen, J., Casal-Lopez, M., Delmastro, G. B., Denys, G. P. J., Dettai, A., Doadrio, I., Kalogianni, E., Kärst, H., Kottelat, M., Kovačić, M., Laporte, M., Lorenzoni, M., &… Freyhof, J. (2014). Spatial heterogeneity in the Mediterranean Biodiversity Hotspot affects barcoding accuracy of its freshwater fishes. *Molecular Ecology Resources*, *14*(6), 1210–1221. https://doi.org/10.1111/1755-0998.122577

Ghanavi, H. R., Gonzalez, E. G., & Doadrio, I. (2016). Phylogenetic relationships of freshwater fishes of the genus *Capoeta* (Actinopterygii, Cyprinidae) in Iran. *Ecology and Evolution*, *6*(22), 8205–8222. https://doi.org/10.1002/ece3.2411

Johari, S. A., Coad, B. W., Mazloomi, S., Kheyri, M., & Asghari, S. (2009). Biological and morphometric characteristics of, *Capoeta fusca*, a cyprinid fish living in the qanats of south Khorasan, Iran: (Osteichthyes: Cyprinidae). *Zoology in the Middle East*, *47*(1), 63–70. https://doi.org/10.1080/09397140.2009.10638348

Jouladeh-Roudbar, A., Eagderi, S., Murillo-Ramos, L., Ghanavi, H. R., & Doadrio, I. (2017). Three new species of algae-scraping cyprinid from Tigris River drainage in Iran (Teleostei: Cyprinidae). *FishTaxa*, *2*(3), 134–155. https://www.biotaxa.org/ft/article/view/2-3-4

Keivany, Y., Nasri, M., Abbasi, K., & Abdoli, A. (2016). *Atlas of inland water fishes of Iran*. Iran Department of Environment Press.

Levin, B. A., Freyhof, J., Lajbner, Z., Perea, S., Abdoli, A., Gaffaroğlu, M., Özuluğ, M., Rubenyan, H. R., Salnikov, V. B., & Doadrio, I. (2012). Phylogenetic relationships of the algae-scraping cyprinid genus *Capoeta* (Teleostei: Cyprinidae). *Molecular Phylogenetics and Evolution*, *62*(1), 542–549. https://doi.org/10.1016/j.ympev.2011.09.004

Perea, S., Böhme, M., Zupančič, P., Freyhof, J., Šanda, R., Özuluğ, M., Abdoli, A., & Doadrio, I. (2010). Phylogenetic relationships and biogeographical patterns in Circum-Mediterranean subfamily Leuciscinae (Teleostei, Cyprinidae) inferred from both mitochondrial and nuclear data. *BMC Evolutionary Biology*, *10*, 265. https://doi.org/10.1186/1471-2148-10-265

Salehi Nejad Ranjbar, V., Teimori, A., Askari Hesni, M., & Lashkari, M. (2016). Comparative morphology of urohyal bone and otolith in taxonomic identification of two Mullet species (Mugilidae: Teleostei) in Persian Gulf. *Taxonomy and Biosystematics*, *8*(29), 13-24. https://doi.org/10.22108/tbj.2016.21535 [In Persian]

Turan, D., Kottelat, M., & Ekmekçi, F. G. (2006). A review of *Capoeta tinca*, with descriptions of two new species from Turkey (Teleostei: Cyprinidae). *Revue Suisse de Zoologie*, *113*(2), 421–436. https://doi.org/10.5962/bhl.part.80358

Turan, D., Kaya, C., Aksu, İ., & Bektaş, Y. (2022). *Paracapoeta*, a new genus of the Cyprinidae from Mesopotamia, Cilicia and Levant (Teleostei, Cypriniformes). *Zoosystematics and Evolution*, *98*(2), 201–212. https://doi.org/10.3897/zse.98.81463

Yazdani, Z., Vatandoust, S., Khayatzadeh, J., & Sarpanah, A. N. (2016). Scientific Finding: Study of some biological indices of the Black fish *Capoeta buhsei* in the Qareh Chay River basin of Saveh. *Iranian Scientific Fisheries Journal*, *25*(3), 257–262. https://doi.org/10.22092/isfj.2017.110275 [In Persian]

Zareian, H., Esmaeili, H. R., & Freyhof, J. (2016). *Capoeta anamisensis*, a new species from the Minab and Hasan Langhi River drainages in Iran (Teleostei: Cyprinidae). *Zootaxa*, *4083*(1), 126-142. https://doi.org/10.11646/zootaxa.4083.1.6

Zareian, H., Esmaeili, H. R., Gholamhosseini, A., & Freyhof, J. (2018). Diversity, mitochondrial phylogeny, and ichthyogeography of the *Capoeta capoeta* complex (Teleostei: Cyprinidae). *Hydrobiologia*, *806*, 363-409. https://doi.org/10.1007/s10750-017-3375-0